Probing Interdomain Mixing Effects via Specific Interactions: A Model System Approach

Ralph E. Taylor-Smith and Richard A. Register*

Department of Chemical Engineering, Princeton University, Princeton, New Jersey 08544

Received January 29, 1993

ABSTRACT: The feasibility of applying specific interactions to promote interdomain adhesion in multicomponent materials was investigated using a model bicomponent system. Polystyrene (with either phenolic or sulfonic functionality at variable levels) and poly(ethyl acrylate) form the basis of our system, with adhesion arising from intercomponent mixing at the domain interface. The driving force for mixing was confirmed via infrared spectroscopy to be hydrogen bonding between the styrene acidic functions and the acrylate carbonyl. We demonstrate that the degree of mixing can be varied continuously in these multiphase materials via systematic control of the polystyrene functionalization level, and we probe the macroscopic effects of enhanced intercomponent adhesion via thermal, thermomechanical, and uniaxial tensile stress–strain analyses. At high functionalization levels, contrasting trends are evident in the activity of the two compatibilizing functions used. Component segregation is observed when the polystyrene is sulfonated, with adverse consequences on blend mechanical properties, but not when the polystyrene contains phenolic units. Free energy computations based upon the association model of Coleman, Painter, and co-workers suggest the observed segregation is driven by the dominance of dispersive interactions.

I. Introduction

Mixtures of most polymers form incompatible blends.[1] There is little intermixing of components, leading to a domain structure with sharp domain interfaces. Consequently, interfacial adhesion is poor, as there is inefficient stress transfer across domain boundaries.[2] The result is generally imperfect mechanical properties, with premature material failure localized at the domain interface. This study focuses on the application of specific interactions (intermolecular hydrogen bonds) to enhance interfacial adhesion in multiphase polymeric systems, partially offsetting intramolecular cohesive forces of individual components via "interfacial mixing". This term describes intermixing of polymer components that is localized primarily at domain boundaries, providing a graded transition between domains of differing composition. Such interdomain mixing effects can be induced via interactions between functional groups on respective polymer components in what is often referred to as a functionalized blend. With a small number of interacting sites, enthalpic considerations dictate that these interactions would be localized at the domain interface, promoting entanglements between dissimilar chains due to their interpenetration. Such localized segmental mixing would augment the interphase, thus ensuring adhesion. The expected macroscopic result would be enhanced mechanical response, particularly in the large strain behavior and ultimate properties where interdomain adhesion is most critical.

In recent years, a large number of studies have been documented on the development of miscible blends through specific interactions. Drawing from the literature, in particular the work of Eisenberg and co-workers,[3-6] Coleman, Painter, and co-workers,[7,8] and MacKnight and co-workers,[9,10] we have generated a model system, based upon a series of bicomponent polymer blends, that permits us to investigate quantitatively the interrelationships that exist between microscopic interfacial mixing and the resultant macroscopic mechanical response. The emphasis is on a blend system based upon a glassy polymer, polystyrene or PS, and a rubbery polymer, poly(ethyl acrylate) or PEA. Interdomain mixing is induced via the systematic introduction of acidic moieties (phenolic and sulfonic acid groups) at variable levels onto the PS component through postpolymerization techniques, the acidic units being randomly distributed along the PS chain. From documented studies,[7,11,12] we anticipate hydrogen bonding interactions between the PS acidic functions and the PEA carbonyl upon blending, the resultant materials exhibiting a range of interfacial mixing, controlled by the PS functionalization level and type. A single precursor batch is used for the preparation of samples of differing functionalization level, eliminating any encumbering effects of molecular architecture. The small fraction of acidic sites introduced (<8% of PS repeat units) minimizes variances in the glass transition temperature (T_g) and other physical properties of the glassy component. Thus, any changes in mechanical properties with functionalization level are solely the result of changes in miscibility.

In this report, all blends were prepared at a 50:50 weight ratio, to promote formation of a cocontinuous morphology in which the glassy phase would bear most of the stress at small strains. At high strains, when the glassy phase has lost continuity, the behavior should strongly reflect the quality of adhesion between glassy and rubbery domains. In future work, we will examine the behavior of blends with asymmetric compositions, particularly those with discontinuous rubbery phases.

II. Experimental Section

A. Sample Preparation. PEA (see Figure 1) was synthesized via free radical polymerization of ethyl acrylate (99%, Aldrich) in benzene solution (1/4, v/v) at 50 °C with 1.3×10^{-3} M of azobis(isobutyronitrile) as initiator. Before polymerization, the monomer was deinhibited by passing it through the appropriate inhibitor removal column (Aldrich). The reaction was terminated at approximately 50% conversion; the product had a zero-shear-corrected intrinsic viscosity (trichloromethane, 30 °C) of 7.2 dL/g, corresponding to a number-average molecular weight[13] of approximately 2.6×10^6 g/mol.

Lightly sulfonated polystyrene or SPS (see Figure 1) of varying sulfonate content was prepared via reaction of a single well-characterized PS precursor batch ($M_w = 2.99 \times 10^5$, $M_w/M_n = 2.4$ by GPC) with acetyl sulfate in 1,2-dichloroethane solution.[14,15] Monomeric acid byproducts were removed by Soxhlet extraction with water for about 1 week, until the extract titrated neutral.

* To whom correspondence should be addressed.

0024-9297/93/2226-2802$04.00/0

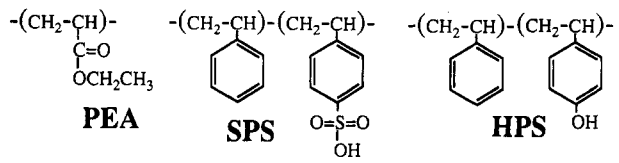

Figure 1. Structure of blend components.

The sulfonation level was determined via elemental analysis for sulfur (Galbraith Laboratories, Knoxville, TN). The functionalization route used is known to be relatively free from side reactions, with no substantial effect on chain architecture.[14] For comparison, fully-sulfonated poly(styrenesulfonic acid) was obtained from Polysciences.

Lightly hydroxylated polystyrene or HPS (see Figure 1) of varying hydroxyl (phenol) content was prepared via a two-step procedure. Firstly, a single batch of styrene-*co*-*p*-acetoxystyrene was synthesized via free radical copolymerization in benzene at 60 °C (30:70 monomer:solvent, v/v) with 2.1×10^{-4} M of benzoyl peroxide as initiator. Before polymerization, the styrene (99%, Aldrich) was deinhibited by passing it through the appropriate inhibitor removal column (Aldrich); the *p*-acetoxystyrene (gift of Hoechst Celanese, inhibited with 25 ppm phenothiazine) was used as received. Reactivity ratios for this copolymer system (values for styrene:acetoxystyrene are 0.88:1.18 respectively)[16,17] are such that compositional drift is negligible at low conversions. The starting monomer ratio was that computed to produce 7 mol % *p*-acetoxystyrene content. The reaction was terminated at approximately 20% conversion by precipitation into methanol; GPC analysis yielded $M_w = 5.0 \times 10^5$, $M_w/M_n = 1.8$ (polystyrene-equivalent values). Analysis by ^{1}H NMR indicated a *p*-acetoxystyrene content of 6.95 mol %. Samples from this precursor batch were treated with hydrazine[11,16] (2% w/w polymer in 1,4-dioxane, 25 °C, 5:1 mole ratio of hydrazine:acetoxy) to cleave the acetoxy groups to varying extents, yielding phenolic hydroxyl groups. The hydroxyl content was controlled by varying the reaction time from 0 to 35 h, and the extent of reaction was monitored by Fourier transform infrared (FTIR) spectroscopy (acetoxy C=O, 1765 cm^{-1}). To check for any chain cleavage or cross-linking, intrinsic viscosity measurements were performed before and after hydrazinolysis; 2-butanone was chosen as the solvent in an attempt to disrupt hydrogen bonding between phenol groups in the product. The [η] values were 0.78 dL/g before hydrazinolysis and 0.74 dL/g after, so we deduce that the hydrazinolysis reaction had no deleterious effects on molecular architecture. For comparison, fully-functionalized poly(vinylphenol) was provided by Hoechst Celanese.

Blends were prepared by dissolving equal weights of PEA and SPS or HPS in 1,4-dioxane to obtain 2% solutions at 25 °C. The solutions were frozen in liquid nitrogen, and the solvent was removed via freeze-drying at 0 °C. Resulting materials were compression-molded at 120–140 °C into films for analysis. Freeze-drying was chosen as a blend preparation method because it should produce an initially intimate mixture of the two components; any phase separation would thus develop from an initially homogeneous material.

B. Sample Analysis. Gel permeation chromatography (GPC) was performed in toluene at 1.0 mL/min using a Polymer Laboratories Mixed-C column (60 cm) and a Knauer refractive index detector. The molecular weight was calibrated with narrow-dispersity polystyrene standards. Differential scanning calorimetry (DSC) measurements were conducted with a Perkin-Elmer DSC-4, calibrated with indium, at a heating rate of 20 °C/min under nitrogen atmosphere. FTIR absorbance spectra were obtained on a Nicolet 730 spectrophotometer under nitrogen purge at 25 °C. Samples for infrared analysis were prepared via compression molding into sufficiently thin films. Dynamic mechanical thermal analysis (DMTA) measurements at 1 Hz employed a Rheometrics RSA-II (fiber-film geometry) performed under nitrogen atmosphere. To maintain sample compliance within the instrument's range, data were collected over several temperature ranges using films of different thicknesses and spliced together.

Uniaxial tensile stress–strain measurements were obtained at room temperature on an Instron TM-SM at a crosshead speed of 5 cm/min, utilizing samples stamped from molded films with an ASTM D1708 die. Permanent set measurements were obtained by elongating a sample to 100% strain, again at a crosshead speed of 5 cm/min at room temperature, unloading, and permitting relaxation to occur for 30 min. The permanent set was recorded as the final percent strain. Reported data are an average of three to five tests.

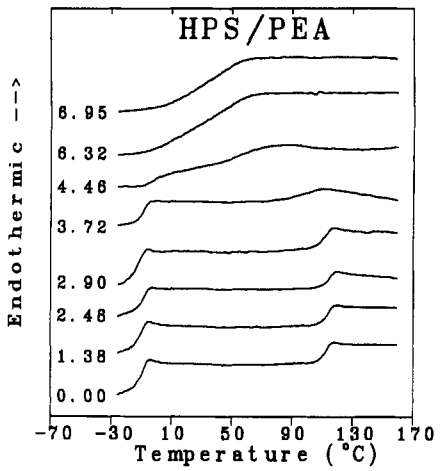

Figure 2. DSC data for the HPS/PEA blend series. Numbers indicate the mole percent of styrene units functionalized.

III. Results and Discussion

Both the SPS/PEA and HPS/PEA blend series produced optically clear molded films at and above 5 mol % PS functionalization level, indicating that, at the higher functionalities, any phase separation present was confined to submicron domains.

A. Differential Scanning Calorimetry (DSC). It has been well documented[18,19] that information regarding the type and extent of phase mixing can be extracted from an analysis of the shifts and broadenings of glass transitions in multiphase polymeric systems. Interfacial mixing is manifested as a broadening of transitions toward each other, with little shift in the temperature extremes of the transitions relative to those of the pure components. In contrast, in-domain mixing (where the composition of each domain is uniform but not pure, and the interface remains relatively sharp) is characterized by relatively narrow transitions which are shifted substantially from those of the pure components. Both of these mixing phenomena are clearly evident in the DSC data. In the HPS/PEA data set (Figure 2), the unfunctionalized material (0.00%) shows two sharp well-separated glass transitions, characteristic of an incompatible blend. However, as the functionalization level is increased, the transitions gradually broaden toward each other with initially little shift in position, an indication that mixing is primarily interfacial. In particular, note the DSC scan for the 4.46% HPS/PEA sample which shows very broad transitions. At higher PS functionality, the effect of in-domain mixing becomes more pronounced and the two transitions coalesce to form one single broad transition, characteristic of a blend approaching miscibility.

Data for the SPS/PEA blend series, shown in Figure 3, are very similar to that described above for HPS/PEA at low functionalization levels. However, as the functionality is increased further, the transition does not sharpen to the same extent as in the HPS/PEA blends, suggesting that a reduced level of miscibility is obtained in the SPS/PEA blends at comparable functionalization levels.

B. Fourier Transform Infrared Spectroscopy (FTIR). On the basis of the functional groups present in the blend constituents, we expected hydrogen bonding between acidic protons of the functionalized PS and the

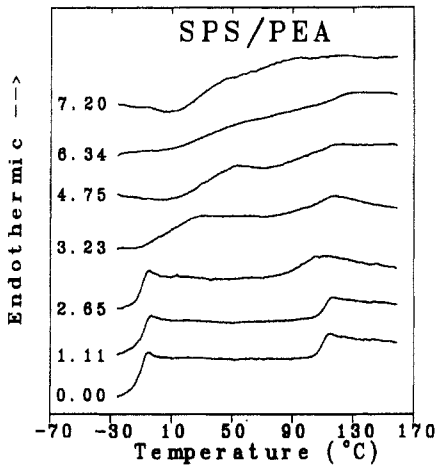

Figure 3. DSC data for the SPS/PEA blend series. Numbers indicate the mole percent of styrene units functionalized.

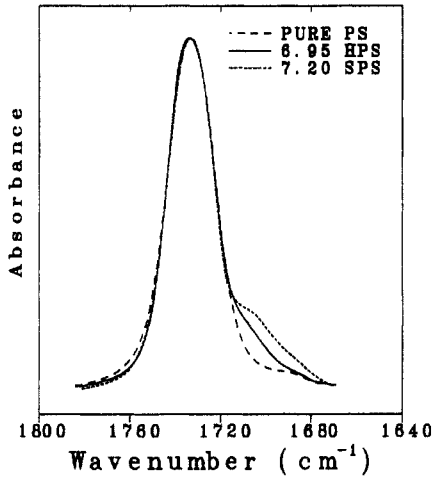

Figure 4. FTIR spectra, scale-expanded to show the carbonyl absorption region. All spectra are of 50/50 w/w PS/PEA blends, with differing functional groups on the PS: (- - -) unfunctionalized PS; (—) 6.95 mol % HPS; (···) 7.20 mol % SPS.

PEA acrylate carbonyl to be the driving force for mixing in this system. Direct confirmation of the occurrence of hydrogen bonding was obtained via FTIR. The use of infrared spectroscopy to detect and quantify intermolecular interactions in multicomponent systems is now well-established. The interested reader is directed to a well-written expansive review of the topic.[20] Figure 4 shows FTIR spectra for the most highly functionalized blend in each series, scale-expanded to display the carbonyl absorption region. The analogous spectrum for a blend of "pure" or unfunctionalized PS/PEA is included for comparison. All three spectra show an intense peak centered about 1734 cm^{-1}. Those of the functionalized blends also exhibit a clear shoulder which spectral subtraction shows to be centered near 1706 cm^{-1}. On the basis of the results of previous investigators,[20,21] we assign these absorptions to "free" and "hydrogen-bound" carbonyl groups, respectively. Spectroscopic studies on systems similar to HPS/PEA have been extensively documented by Coleman, Painter, and co-workers.[21] Extracting their value for the appropriate absorption coefficient ratio ($a_{H\text{-bound}}/a_{free}$ = 1.5), we compute from the 6.95% HPS/PEA spectrum shown in Figure 4 that 3.4% of the acrylate carbonyls are hydrogen-bound for this particular blend. This translates to approximately half (52%) of the phenolic groups interacting with a carbonyl.

One final point to note from the infrared data concerns the relative strength of the hydrogen bond formed between

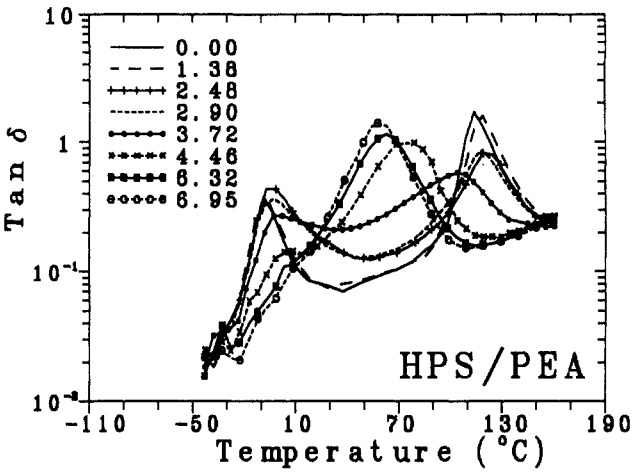

Figure 5. DMTA loss tangent data for the HPS/PEA blend series. Numbers indicate the mole percent of styrene units functionalized.

the acrylate carbonyl and respective acidic functional groups. Information regarding the relative strength of specific intermolecular interactions can be obtained from infrared spectroscopic studies, via a correlation of the wavenumber shift of the absorption band of the interacting species (in this case, the acrylate carbonyl) relative to that of the corresponding "free" species;[12] the greater the shift, the stronger the interaction. This evidence is never absolutely conclusive due to a number of complicating factors;[20] however, it serves as a good first approximation. Since the peaks producing the "hydrogen-bound" shoulders are both centered at about 1706 cm^{-1}, the wavenumber shift is about the same for both HPS/PEA and SPS/PEA. This is a good indication that the phenol–carbonyl interaction and the sulfonic acid–carbonyl interaction are of comparable strength.

C. Dynamic Mechanical Thermal Analysis (DMTA). DMTA loss tangent (tan δ) data for the HPS/PEA blend series are displayed in Figure 5. As with the DSC data, the location and shape of the blend transitions provide some insight into the morphology; the gradual broadening effect with increasing functionality is even more obvious in the DMTA data. In Figure 5, the curve for the 3.72% HPS/PEA sample clearly shows enhanced interfacial mixing (very broad transitions), but the material is still two-phase (two resolvable peaks). As the functionalization level is increased further to 4.46%, there is an obvious change in the shape of the tan δ curves. While a small low-temperature shoulder is still evident, most of the area of the tan δ curve occurs under a large peak at a temperature intermediate between the two pure-component glass transitions. We interpret this to mean that, in the 4.46% HPS/PEA blend, most of the material exists in a mixed phase, with a tan δ maximum at about 75 °C, while only a small amount of a PEA-rich phase remains. This would suggest that the rubbery phase ceases to be continuous at about 4% functionalization, a point which will be addressed below. As the functionalization is increased further, to levels higher than 4.46%, in-domain mixing effects become more pronounced. The initially broad transition narrows, becoming more well-defined as the blend approaches miscibility, while the low-temperature shoulder becomes undetectable.

At low functionalization levels, the SPS/PEA loss tangent data, displayed in Figure 6, follow the same trend as those for the HPS/PEA and a similar shape change in tan δ is observed between 3.23% and 4.75% functionalization. However, in sharp contrast with the HPS/PEA

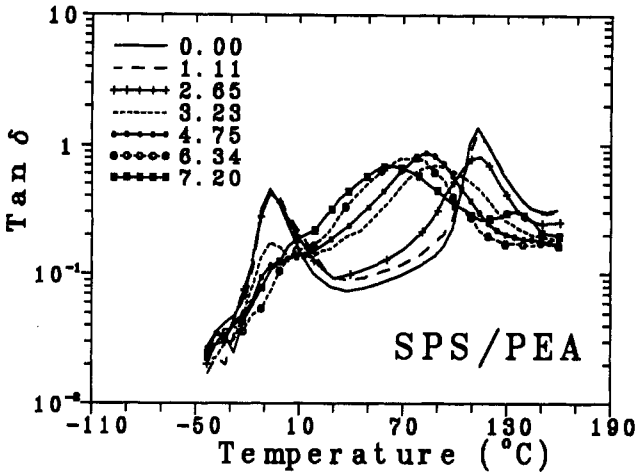

Figure 6. DMTA loss tangent data for the SPS/PEA blend series. Numbers indicate the mole percent of styrene units functionalized.

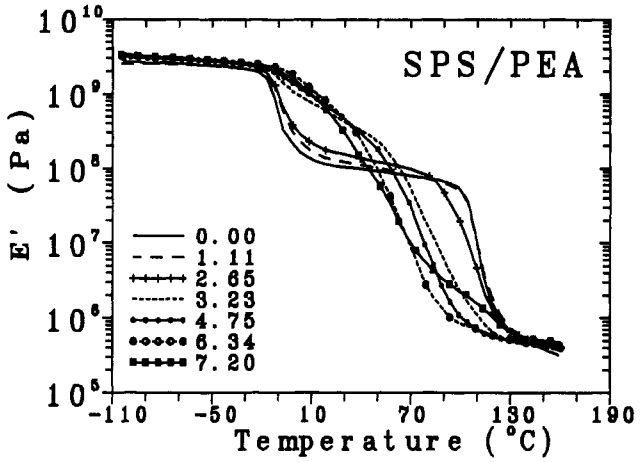

Figure 7. DMTA storage modulus data for the SPS/PEA blend series. Numbers indicate the mole percent of styrene units functionalized.

blend series, as the functionality is increased to higher levels we do not see the same miscibility-enhancing effects. Instead, the transition broadens, particularly at the low-temperature end, implying a more heterogeneous PEA-rich phase (demixing), and at our highest functionalization level (7.20%), an additional high-temperature relaxation appears, centered about 130 °C. Since this temperature is comparable to the glass transition temperature of pure SPS of the appropriate sulfonate content, we infer that some component segregation occurs at the higher functionalities for the SPS/PEA blend series. Annealing experiments on the most highly functionalized sample (7.20% SPS/PEA) showed that these phase separation effects were even more prominent with higher annealing temperatures and longer annealing times. The additional high-temperature relaxation grew in magnitude at the expense of the major broad transition. Component segregation in the SPS/PEA series at high functionalities is also clearly evident in DMTA storage modulus (E') data shown in Figure 7. Again, we see the appearance of an additional high-temperature relaxation for the 7.20% SPS/PEA sample. Analogous DMTA storage modulus data for the HPS/PEA series are displayed in Figure 8; as with the loss tangent data, we see no phase separation effects at high functionalities. This contrast results in acute differences in mechanical response between the HPS/PEA and SPS/PEA blend series at high functionalities, as will be discussed below. However, both data sets show similarities in the manner in which the E' curves are shifted

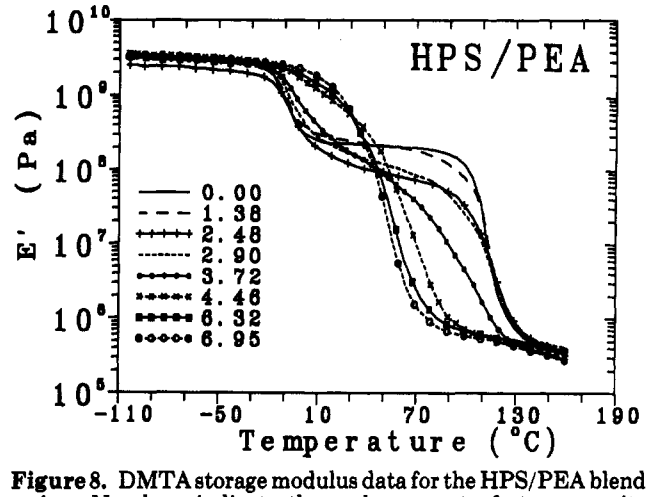

Figure 8. DMTA storage modulus data for the HPS/PEA blend series. Numbers indicate the mole percent of styrene units functionalized.

and broadened as a reflection of the mixed environment. Interfacial mixing is manifested as the "smoothing-out" of the intermediate step between the high- and low-temperature plateau regions, a clear illustration of the graded transition between unlike domains. This feature dominates the appearance of the E' curves with increasing functionality until in-domain mixing effects become more pronounced and a single step emerges.

D. Tensile Testing. One would expect the mechanical properties of these rubbery–glassy multicomponent materials to be influenced by several factors: in particular, domain size, domain connectivity, and glass–rubber domain adhesion. Documented work on rubber-toughened plastics has shown some dependence of domain size on mechanical properties.[22] However in this study, domain size cannot be independently controlled. In a simplified scenario, characteristic dimensions would necessarily decrease as the functionality increased so as to maximize interactions. We have attempted to diminish the effect of domain size by maintaining the blend ratio at 50/50. This should promote a cocontinuous domain structure in which large-strain tensile behavior should be dictated primarily by interfacial adhesion. Scanning electron microscopy has been used to characterize the materials described in this study,[23] and it was determined that at the low end of the functionality range, the materials clearly exhibit a cocontinuous interconnected domain morphology.

Figure 9 shows uniaxial tensile stress–strain data for the HPS/PEA blend series; analogous data for SPS/PEA are shown in Figure 10. Dramatic changes in mechanical properties are observed with increasing functionality. In Figure 9, as the functionalization level increases, we observe a corresponding increase in ultimate stress as interfacial adhesion is enhanced. The elongation-to-break also drops initially (less creep) as a consequence, since the rubbery PEA chains are increasingly anchored by the glassy domains. But, more importantly, as the morphology changes from predominantly a two-phase material (with a significant fraction of the blend possessing a T_g below ambient temperature) to predominantly a one-phase material (where most of the material has a T_g above ambient), there is a corresponding change in the stress–strain behavior. A monotonically increasing stress–strain curve at 3.72% HPS/PEA is replaced by one with a distinct yield point at 4.46% HPS/PEA. As the functionality is increased further, the yield point becomes sharper and better-defined but all other features of the mechanical response remain approximately constant.

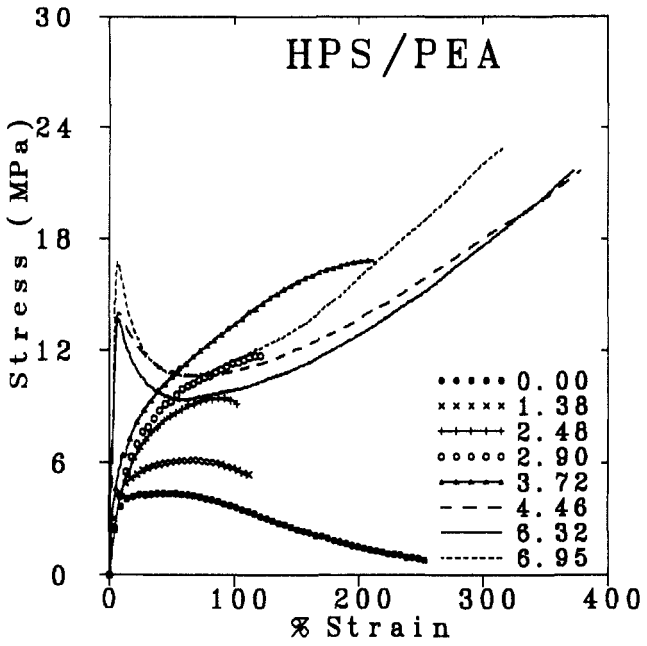

Figure 9. Uniaxial tensile stress–strain data for the HPS/PEA blend series. Numbers indicate the mole percent of styrene units functionalized.

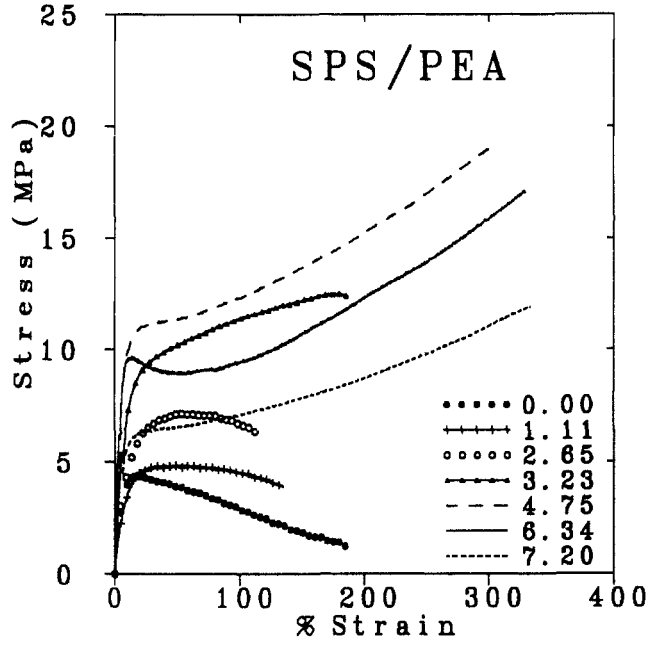

Figure 10. Uniaxial tensile stress–strain data for the SPS/PEA blend series. Numbers indicate the mole percent of styrene units functionalized.

The stress–strain behavior of the SPS/PEA series, displayed in Figure 10, is similar to that of the HPS/PEA series up to 4.75% functionalization. However, as the functionalization level is increased further, the mechanical behavior departs from the trend observed for the HPS/PEA materials. The yield point does not become quite as distinct, while the modulus and ultimate stress decrease significantly. Figure 11 shows Young's modulus and ultimate stress values plotted versus functionality for each blend series. For both HPS/PEA and SPS/PEA at low functionalities, Young's modulus is approximately constant, while the ultimate stress increases monotonically. Constancy of modulus indicates little change in the domain continuity, while the increase in ultimate stress is due to improved adhesion between the two phases. At about 4% functionalization, corresponding to the point where

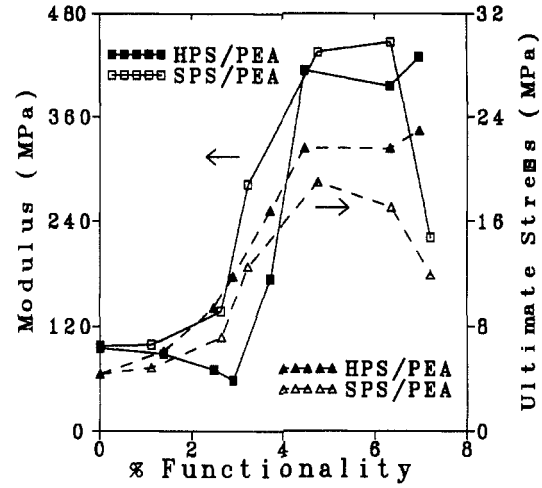

Figure 11. Young's modulus (squares, solid lines) and ultimate stress values (triangles, dashed lines) extracted from the stress–strain data.

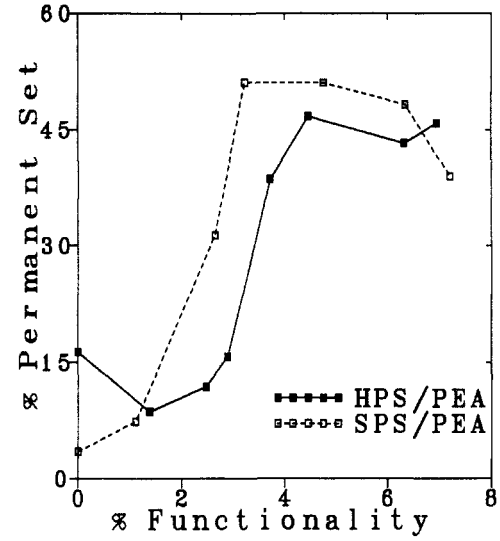

Figure 12. Permanent set results (100% strain).

DMTA indicated a sudden drop in the amount of low-T_g phase, sudden increases in both the modulus and ultimate stress are observed. Such a response is expected if indeed the morphology transforms from a cocontinuous rubber–glass domain structure to one in which the rubber phase is discontinuous but possesses good adhesion to the glassy phase.

With increasing functionality, the mechanical response of HPS/PEA and SPS/PEA deviate in trend. For the HPS/PEA, both modulus and ultimate stress plateau, remaining approximately constant. Considering the minor changes in tan δ data for this series at the higher functionalities, the trend is not surprising. For the SPS/PEA, both modulus and ultimate stress decrease with increasing functionality. This is a result of the phase separation effects that are observed in the DMTA data for this blend series, with an increase in the fraction of low-T_g material at higher functionalization levels. Exactly the same trends are seen in permanent set measurements for these materials, shown in Figure 12. At low functionalities, the permanent set is low as the materials exhibit significant rubbery character. Near 4% functionality, the permanent set increases dramatically, and at high functionality, it plateaus for the HPS/PEA series but decreases slightly for SPS/PEA.

Mechanical behavior grossly similar to that described here has been documented in the literature[24] for segmented

polyether–polyurethane copolymers of variable hard segment content, where hydrogen bonding can occur between hard and soft segments. With increasing hard segment content, and thus increasing interconnectivity of hard domains, a yield point appears in the stress–strain curve and there are substantial increases in modulus, ultimate stress, and toughness as the material changes from predominantly soft segment to predominantly hard segment. However, that system is more complicated than the one described here, as those authors have crystallinity of the hard segments to contend with and, in addition, a possibility of strain-induced soft segment crystallization.

E. Free Energy Computations. The original impetus for utilizing both phenolic and sulfonic acid groups as interfacial compatibilizers was to compare the macroscopic effects of weak and strong compatibilizing agents. Our rationale here was that a comparison of appropriate small molecule analogs (phenol and benzenesulfonic acid) implied a significant difference in acidity and hence proton donating capacity. Thus, we inferred a concomitant disparity in relative compatibilizing power. However, the thermal and mechanical analyses described above proved that this is not the case. At low functionalities (below about 5%), HPS and SPS are equivalent as compatibilizing agents. It is obvious from this that proton donor acidity is not the sole factor determining compatibilizing activity. Other more subtle factors must contribute. This phenomenon has been documented before,[11] and it has been suggested that an additional consideration may be the basicity of the proton acceptor relative to that of the proton donor,[12] which would impact on the competition between adhesion-enhancing cross-associations and adhesion-negating self-association of the proton donor.

At higher functionalities, HPS and SPS differ in compatibilizing activity due to segregation of the SPS component. We believe that the phase separation effects observed are due to the prevailing influence of dispersive forces, the strength of which would increase with increasing polar character and hence the functionality of the PS component. If the compatibilizing moiety were sufficiently polar, there might be some functionalization level where dispersive interactions would be of sufficient strength so as to overwhelm interactions due to hydrogen bonding, leading to a decrease in miscibility. These ideas prompted us to investigate the miscibility of blends with the appropriate "fully-functionalized" analogs of HPS and SPS, namely poly(vinylphenol) or PVPH and poly(styrenesulfonic acid) or PSSA. Since sulfonic acid is more polar than phenol ($\delta_{SSA} > \delta_{VPH}$) and our experimental observations already indicate demixing of the SPS/PEA blends at the highest functionalization levels, we speculated that the blend with PSSA might be immiscible while that with PVPH might be miscible. DSC studies on 50:50 blends of poly(ethyl acrylate) with commercially available samples of PSSA and PVPH confirm these predictions. For the blend with PSSA, we obtained two glass transitions, almost identical in breadth and location to those of the pure components, while the data for the PVPH blend (in affirmance of earlier work[7]) yielded one distinct narrow transition, intermediate between those of the pure components. This experimental evidence seemed to support our qualitative arguments.

In search of a quantitative framework in which to interpret our results, we turned to the association model derived by Coleman, Painter, and co-workers[25,26] to describe free energy changes in blend systems where hydrogen bonding occurs between polymer components. Its authors have documented its successful application to various homopolymer[7] and copolymer[8,27,28] blend systems; we apply their general methodology to predict the mixing thermodynamics for our system. Employing the governing equations documented in the literature,[25] we utilize the two-equilibrium-constant approach to describe self-association of the proton donating species, with one constant for dimer formation and another for multimer formation. A third equilibrium constant is used to describe cross-associations. Relevant imput parameters for the model are given in Table I. Solubility parameters for the proton donating copolymer were determined for differing functionalities applying standard methods[8,28] and used to compute dispersive interaction parameters. To more accurately represent our experimental system, the calculated solubility parameter for the HPS component included a contribution from unhydrazinolyzed acetoxy groups for functionalities below 6.95%, such that the sum of acetoxy and hydroxyl functionality totaled 6.95 mol %; above this level, the solubility parameter was that calculated for a styrene–vinylphenol copolymer. Thus, the calculated dispersive free energy contribution for the HPS/PEA system should match our experimental system over the range in which data were obtained (up to 6.95% functionalization).

Table I. Parameter List[a]

polymer	solubility param δ (cal/cm^3)$^{0.5}$	repeat unit molar vol (cm^3/mol)
polystyrene	9.20	98.0
poly(ethyl acrylate)	9.52	86.6
poly(*p*-acetoxystyrene)	10.29	128.6
poly(vinylphenol)	10.89	100.5
poly(styrenesulfonic acid)	15.35*	148.9*

[a] Values obtained via group contribution methods from correlations by Coleman, Painter, and co-workers,[29] except those marked * from correlations by Fedors.[30]

Because the HPS component contains acetoxy groups at all but the highest functionalization level, and since these acetoxy groups can act as acceptors for the phenolic –OH, we considered that association between these groups (which would satisfy the phenol's tendency to hydrogen bond, but not promote miscibility with the PEA) might occur. To investigate this, we performed FTIR studies on the unblended HPS copolymers; even at the higher levels of acetoxy content, less than one in seven phenols was bound to an acetoxy carbonyl. Thus, there is some justification in neglecting any contribution of acetoxy groups to the hydrogen bonding part of the free energy of mixing. Further confirmation was obtained by performing DSC measurements on fully-hydrazinolyzed HPS polymers (of varying *p*-acetoxystyrene content) synthesized by the same general method, blended in a 50:50 ratio with PEA. The positions and breadths of the transitions were in good agreement with those observed for the HPS/PEA system, implying that acetoxy groups do not discernably affect the extent of cross-association between phenolic hydroxyl and acrylate carbonyl.

Values for the degree of polymerization of the proton donating component represent realistic estimations determined from the molecular weight of the unfunctionalized precusors ($N_{HPS} = 5000$, $N_{SPS} = 3000$). That for the proton acceptor component was simply determined from its molecular weight ($N_{PEA} = 26\,000$). Appropriate interaction equilibrium constants and enthalpies used are shown in Table II. These values are specific to the HPS/PEA blend series; we were unable to find appropriate literature values for the SPS/PEA series, and thus we have applied these values to both series. This should provide a rough estimate of the SPS/PEA mixing thermodynamics

Table II. Poly(vinylphenol)/Polyacrylate Interaction Constants[7]

interaction type	equilibrium constant (25 °C)	enthalpy (kcal/mol)
self-association (dimer)	21.6	5.6
self-association (multimer)	68.6	5.2
cross-association	50.0	4.3

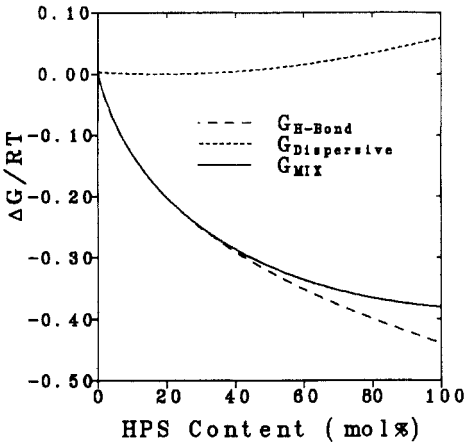

Figure 13. Calculated free energy of mixing contributions for HPS/PEA.

since the FTIR studies discussed above (see section III.B) indicate that the phenol–carbonyl and the sulfonic acid–carbonyl interactions are of comparable strength. As in previous studies,[7,8] a van't Hoff expression was used to scale interaction constants to the appropriate temperature: 120 °C, the condition at which most compression-molded samples were prepared.

Some modifications were made to the general approach outlined by Coleman, Painter, and co-workers,[7,8,25] particularly in the computation of the dispersive contribution (see eq III of ref 7) to the free energy of mixing. Firstly, the entropic portion of the dispersive contribution was calculated using the fixed values of polymerization index N listed above, rather than basing N on an average repeat unit containing a single functional group. (Because our polymers have large N values, the entropic contribution was much smaller than the other terms.) Secondly, the enthalpic portion of the dispersive contribution was computed over the range of functionalities with a dispersive interaction parameter (see ref 7) based upon a constant reference volume ($V_B = V_{PS} = 98.0$ cm^3/mol) instead of a variable volume containing a single functional group. These two modifications reduced the form of the dispersive free energy change to that obtained from the Flory–Huggins theory, thus eliminating a physically unrealistic divergence in the dispersive contribution as the functionality decreased to zero. Thirdly, for the hydrogen bonding contribution, we followed the treatment wherein the lattice cell size is defined by an "interacting segment", which varies continuously with functionalization level. We took the parameter S_B (eq 38 in ref 25) to equal the interacting segment volume (average volume of segments containing one functional group) normalized by the volume of the interacting repeat unit (vinylphenol or styrenesulfonic acid). This modification also removes a divergence as the functionality approaches zero.

Figure 13 shows the free energy contributions for HPS/PEA; analogous results for the SPS/PEA are displayed in Figure 14. The hydrogen bonding contribution to the free energy of mixing, $G_{H\text{-bond}}$, becomes more negative with increasing functionality due to the increasing concentration of proton donors. The dispersive contribution,

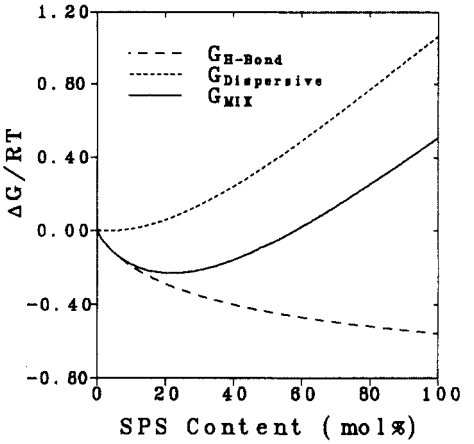

Figure 14. Calculated free energy of mixing contributions for SPS/PEA.

$G_{Dispersive}$, decreases initially and then increases, as the solubility parameter of the styrene component increases from below that of PEA to above (δ_{SSA}, $\delta_{VPH} > \delta_{PEA} > \delta_{PS}$). The balance of these two contributions is the equilibrium free energy of mixing, G_{MIX}. For HPS/PEA, there is qualitative agreement between the model results and our data; however quantitative agreement is poor. Under equilibrium conditions, HPS/PEA is predicted to become miscible at relatively low functionality (~0.06%) and remain miscible with increasing functionality. While the mixing behavior predicted is similar to that experimentally observed, the functionality at which miscibility is achieved (~5%) is not accurately generated by the model. For SPS/PEA, quantitative agreement was not expected since the proper interaction equilibrium constants and enthalpies are unknown. Again however, the qualitative trend predicted is the same as that experimentally observed. Mixing is predicted to occur at relatively low functionality (~0.07%) but then is disfavored at higher functionality (~58%) due to the dominance of dispersive interactions. Specific reasons for the quantitative discrepancy between the association model's predictions and experiment remain unclear. It seems certain that for copolymer blends particularly at the low end of the functionality range, contributions to the free energy of mixing are not adequately generated. This discrepancy is probably not due to the dispersive free energy contribution; although literature values for the appropriate solubility parameters vary, no PS/PEA solubility parameter difference based on literature values could produce a $G_{Dispersive}$ sufficiently large to bring the calculated miscibility points in line with experiment. Therefore, the failing appears to be in the calculation of the hydrogen bonding contribution. Nevertheless, the predicted trends are correct and qualitative agreement is achieved at the functionality end points (homopolymer blends).

IV. Conclusions

Interdomain mixing was induced via specific interactions in a model multiphase system, and its effects on thermal and mechanical properties were probed experimentally by DSC, FTIR, DMTA, and uniaxial tensile stress–strain measurements. The presence of hydrogen bonding interactions was verified via infrared spectroscopy. Thermal and thermomechanical analyses provided vivid insight into the degree of intercomponent mixing, both in-domain and interfacial, that can be promoted through intermolecular interactions and the level of control and specificity that is achievable via the functionalization approach.

Macroscopic effects of interdomain mixing were patently evident in the stress–strain and strain hysteresis data. In

particular, a transition from a mechanical response with significant rubberlike character to one where plasticlike deformation behavior predominates is observed as the domain composition homogenizes. At higher functionalization levels, contrasting trends are observed for the HPS/PEA and the SPS/PEA blend series. The mechanical response of the SPS/PEA materials becomes significantly poorer than that of the HPS/PEA due to component segregation. Calculations based upon the association model of Coleman, Painter, and co-workers add credence to the premise that segregation is driven by dispersive interactions, which increase in strength with increasing functionality, though quantitative agreement with the miscibility boundaries was not obtained. For a sufficiently polar unit such as sulfonic acid, the possibility exists for dispersive interactions to overwhelm those from hydrogen bonding, inducing macrophase separation, with an adverse effect on mechanical properties.

Acknowledgment. Support for this research from the National Science Foundation, Materials Engineering and Tribology Program (MSS-9108468), is gratefully acknowledged. Fellowship support for R.T.S. has been generously provided by W. R. Grace, PPG Industries, the DuPont Co., and Princeton University.

References and Notes

(1) Olabisi, O.; Robeson, L. M.; Shaw, M. T. *Polymer-Polymer Miscibility*; Academic Press: New York, 1979.
(2) Teyssié, P.; Fayt, R.; Jérôme, R. *Makromol. Chem., Macromol. Symp.* **1988**, *16*, 41.
(3) Natansohn, A.; Murali, R.; Eisenberg, A. *Makromol. Chem., Macromol. Symp.* **1988**, *16*, 175.
(4) Zhang, X.; Eisenberg, A. *J. Polym. Sci., Part B: Polym. Phys.* **1990**, *28*, 1841.
(5) Bazuin, C. G.; Eisenberg, A. *J. Polym. Sci., Part B: Polym. Phys.* **1986**, *24*, 1021.
(6) Smith, P.; Eisenberg, A. *J. Polym. Sci., Polym. Lett. Ed.* **1983**, *21*, 223.
(7) Coleman, M. M.; Lichkus, A. M.; Painter, P. C. *Macromolecules* **1989**, *22*, 586.
(8) Serman, C. J.; Xu, Y.; Painter, P. C.; Coleman, M. M. *Macromolecules* **1989**, *22*, 2015.
(9) Douglas, E. P.; Sakurai, K.; MacKnight, W. J. *Macromolecules* **1991**, *24*, 4575.
(10) Sakurai, K.; Douglas, E. P.; MacKnight, W. J. *Macromolecules* **1992**, *25*, 4506.
(11) Chen, C.; Morawetz, H. *Macromolecules* **1989**, *22*, 159.
(12) Landry, C. J. T.; Teegarden, D. M. *Macromolecules* **1991**, *24*, 4310.
(13) Hachihama, T.; Sumitomo, H. *Tech. Rep.—Osaka Univ.* **1955**, *5*, 485.
(14) Lundberg, R. D.; Makowski, H. S. In *Ions in Polymers*; (*Adv. Chem. Ser. 187*), Eisenberg, A., Ed.; Advances in Chemistry Series 187; American Chemical Society: Washington, DC, 1980.
(15) Register, R. A.; Bell, T. R. *J. Polym. Sci., Part B: Polym. Phys.* **1992**, *30*, 569.
(16) Arshady, R.; Kenner, G. W.; Ledwith, A. *J. Polym. Sci., Polym. Chem. Ed.* **1974**, *12*, 2017.
(17) Brown, D.; Czerwinski, W.; Disselhoff, G.; Tüdös, F.; Kelen, T.; Turcsányi, B. *Agnew. Makromol. Chem.* **1984**, *125*, 161.
(18) Annighofer, F.; Gronski, W. *Colloid Polym. Sci.* **1983**, *261*, 15.
(19) Hashimoto, T.; Tsukahara, Y.; Tachi, K.; Kawai, H. *Macromolecules* **1989**, *22*, 4631.
(20) Coleman, M. M.; Painter, P. C. *Appl. Spectrosc. Rev.* **1984**, *20* (3 & 4), 255.
(21) Moskala, E. J.; Howe, S. E.; Painter, P. C.; Coleman, M. M. *Macromolecules* **1984**, *17*, 1671.
(22) Argon, A. S.; Cohen, R. E. *Adv. Polym. Sci.* **1990**, *91/92*, 301.
(23) Taylor-Smith, R. E.; Register, R. A. To be published.
(24) Miller, J. A.; Lin, S. B.; Hwang, K. K. S.; Wu, K. S.; Gibson, P. E.; Cooper, S. L. *Macromolecules* **1985**, *18*, 32.
(25) Painter, P. C.; Park, Y.; Coleman, M. M. *Macromolecules* **1989**, *22*, 570.
(26) Painter, P. C.; Park, Y.; Coleman, M. M. *Macromolecules* **1989**, *22*, 580.
(27) Bhagwagar, D. E.; Painter, P. C.; Coleman, M. M. *Macromolecules* **1992**, *25*, 1361.
(28) Yang, X.; Painter, P. C.; Coleman, M. M.; Pearce, E. M.; Kwei, T. K. *Macromolecules* **1992**, *25*, 2156.
(29) Coleman, M. M.; Serman, C. J.; Bhagwagar, D. E.; Painter, P. C. *Polymer* **1990**, *32*, 1187.
(30) Van Krevelen, P. W. *Properties of Polymers*; Elsevier: Amsterdam, 1990.